


Thermodynamic analysis of the interactions between human ACE2 and spike RBD of Betacoronaviruses (SARS-CoV-1 and SARS-CoV-2)

Agnieszka Rombel-Bryzek¹, Adriana Miller² and Danuta Witkowska³ 

¹ Institute of Medical Sciences, University of Opole, Poland

² Faculty of Chemistry, University of Wrocław, Poland

³ Institute of Health Sciences, University of Opole, Poland

Keywords

binding interactions; human ACE2; isothermal titration calorimetry; receptor-binding domain; SARS-CoV-1; SARS-CoV-2

Correspondence

D. Witkowska, Institute of Health Sciences, University of Opole, Katowicka 68, 45-060 Opole, Poland
Tel: +4877 44 23 54 8
E-mail: danuta.witkowska@uni.opole.pl

There are many scientific reports on the interaction of the SARS-CoV-2 virus S protein (and its RBD) with the human ACE2 receptor protein. However, there are no reliable data on how this interaction differs from the interaction of the receptor binding domain of SARS-CoV-1 with ACE2, in terms of binding strength and changes in reaction enthalpy and entropy. Our studies have revealed these differences and the impact of zinc ions on this interaction. Intriguingly, the binding affinity of both RBDs (of SARS-CoV-1 and of SARS-CoV-2) to the ACE2 receptor protein is almost identical; however, there are some differences in the entropic and enthalpic contributions to these interactions.

(Received 27 May 2022, revised 11 November 2022, accepted 22 November 2022)

doi:10.1002/2211-5463.13525

Edited by Cláudio Soares

Coronaviruses are enveloped, large, moderately pleomorphic, positive-stranded RNA (+ssRNA) viruses [1,2] belonging to the family Coronaviridae [3]. They are divided into four major genera: Alphacoronaviruses, Betacoronaviruses, Gammacoronaviruses, and Deltacoronaviruses [1,3]. Both severe acute respiratory syndrome coronavirus-1 (SARS-CoV-1) and severe acute respiratory syndrome coronavirus-2 (SARS-CoV-2) belong to the genus Betacoronavirus [1,3,4]. SARS-CoV-1 (responsible for the SARS epidemic in 2002–2004) and SARS-CoV-2 (responsible for COVID-19)

share many similarities. Both viruses cause respiratory diseases transmitted by contact with infected individuals [5]. The genomes of SARS-CoV-1 and SARS-CoV-2 have 79.5% sequence identity [6] and encode the non-structural replicase polyprotein, four structural proteins: spike (S), envelope (E), membrane (M), and nucleocapsid (N), and several additional non-structural proteins called accessory proteins [7–9].

Membrane proteins, the most abundant proteins in coronaviruses, are responsible for the shape and size of virions [9,10]. In addition, the M protein is responsible

Abbreviations

CD, circular dichroism; COVID-19, coronavirus disease 2019; hACE2, human angiotensin-converting enzyme 2; HEK, human embryonic kidney; ITC, isothermal titration calorimetry; NTD, N-terminal domain; RBD, receptor-binding domain; RBM, receptor-binding motif; SARS-CoV-1, severe acute respiratory syndrome coronavirus-1; SARS-CoV-2, severe acute respiratory syndrome coronavirus 2; SMD, steered molecular dynamics; TRIS, tris(hydroxymethyl) aminomethane.

for the processing, modification, and transport of many viral compounds, as well as the formation and release of new virions. The M protein of SARS-CoV-2 has 90.5% homology with the M protein of SARS-CoV-1 [10]. The envelope protein is multifunctional and participates in virion particle assembly and budding [9]. The nucleocapsid protein enters the host cell with the coronavirus genetic material and enables replication, RNA transcription, assembly and release of the virus [9]. The N protein of SARS-CoV-2 is approximately 90% similar to the N protein of SARS-CoV-1 [10].

The spike protein (150 kDa) is a highly glycosylated homotrimer [11] that is distributed on the surface of the virion particles and protrudes radially from the viral envelope, forming a “crown-like” structure [7,12]. The S-glycoprotein is a class I fusion protein and is responsible for the binding of the virion to the host receptor, its fusion with it, and entry into the virus [13]. Both SARS-CoV-1 and SARS-CoV-2 utilize angiotensin-converting enzyme 2 (ACE2), an enzyme found on the outer surface of a variety of cells, as their cellular receptor [14–17]. Previous studies have reported that the structure of the SARS-CoV-2 S protein is similar to that of the SARS-CoV-1 S protein [5,18–20].

Each coronavirus spike protein consists of three segments: an ectodomain, a transmembrane anchor, and an intracellular tail [21]. Two subunits can be distinguished in the ectodomain of the S protein [13,22]. The amino-terminal subunit (S1) is responsible for the binding of the virus to the ACE2 receptor, while the carboxyl-terminal subunit (S2) is responsible for the fusion of the virion with the cell membrane, during which it undergoes a conformational change and rejects the S1 subunit [13,22]. The spike proteins of SARS-CoV-1 and SARS-CoV-2 differ in length. The S protein of SARS-CoV-1 contains 1255 amino acid residues [13], while the S protein of SARS-CoV-2 has 1273 amino acid residues [23,24].

The S1 subunit of coronaviruses includes the N-terminal domain (NTD), the receptor-binding domain (RBD), and two subdomains SD1 and SD2 [25], while the S2 subunit contains a fusion peptide and two heptad repeat regions (HR1 and HR2) [13,22,25].

A critical first step for SARS-CoV-1 and SARS-CoV-2 entry into host cells is binding to the ACE2 receptor. A RBD located in the middle region of the S1 subunit specifically recognizes ACE2 and binds to the membrane portion of the receptor’s claw-like structure [4,6,19,24]. The RBD region of SARS-CoV-1 and SARS-CoV-2 has a sequence identity of approximately 73–76% [4]. The overall structure of the RBD of the two viruses is similar. It contains a core and an extended loop called the receptor-binding motif (RBM), which interacts directly

with ACE2 [19,24]. The core of the RBD has a five-stranded antiparallel β -sheet (β 1– β 4 and β 7) and three short α -helices (α 1– α 3), while the RBM is located between the β 4 and β 7 strands and contains the short β 5 and β 6 strands [8,19].

Nevertheless, many findings suggest some internal sequence and structural differences between the RBD of SARS-CoV-1 and SARS-CoV-2 [19]. The RBD of SARS-CoV-1 and SARS-CoV-2 spans full-length amino acid residues 318–510 and 331–524 of the S protein, respectively [8,10].

Recent structural studies show that extensive interactions occur between RBD and ACE2 [18–20,22]. ACE2 is a homodimer, with each monomer containing an N-terminal peptidase domain, a C-terminal collectrin-like domain, a single-pass transmembrane region, and a short cytoplasmic region. The RBD-binding region of ACE2 is located in its N-terminal peptidase domain [20].

Many previous studies reported variations and conformational differences at the interfaces of SARS-CoV-1 and SARS-CoV-2 with the ACE2 receptor [19,20,24].

They showed a higher binding affinity between ACE2 and SARS-CoV-2 S protein than the binding affinity between ACE2 and SARS-CoV-1 S [3,18,26,27].

This is the point where more sophisticated methods could be used. One of these methods is isothermal titration calorimetry (ITC). Indeed, ITC is the most efficient quantitative method for the determination of thermodynamic properties related to the interactions between two molecules.

This study focuses on the analysis of the differences in ACE2 binding by the S protein SARS-CoV-1 and SARS-CoV-2. Thanks to a carefully designed methodology, we were able to obtain reliable data on binding affinity, stoichiometry, binding enthalpy, and entropy for these interactions and hope to draw the correct conclusions. Although COVID-19 is evolving from a pandemic to an endemic disease, Betacoronaviruses can still be dangerous, especially to the elderly and healthcare workers, and it is worthwhile to know as much as possible about their interaction with the human receptor protein [28].

Materials and methods

Materials

Buffers, namely PBS and tris(hydroxymethyl)aminomethane hydrochloride (TRIS-HCl) were purchased from Sigma-Aldrich (St. Louis, MO, USA), NaOH and NaCl were from Chempur (Piekary Śląskie, Poland). All reagents were of analytical grade. Deionized water with a conductivity of no more than $0.06 \mu\text{S}\cdot\text{cm}^{-1}$ was used to prepare all aqueous solutions.

The SARS-CoV-1 spike RBD (RBD^{CoV1}) and SARS-CoV-2 spike RBD (RBD^{CoV2}) proteins were purchased from ABclonal (Woburn, MA, USA) (catalog numbers: RP01299 and RP01258, respectively). Both proteins are His-tagged and produced in the HEK293 cell expression system. The RBD^{CoV1} consists of Arg306-Phe527 from SARS-CoV-1 spike RBD (Accession; [NO_828851.1](#)). The RBD^{CoV2} consists of Arg319-Phe541 from SARS-CoV-2 spike RBD (Accession; [YP_009724390.1](#)) (Fig. 1). The proteins had purity greater than 95% as determined by SDS/PAGE and by HPLC. The human ACE2 protein (hACE2) was purchased from Elabscience (Wuhan, China) (catalog number: PKSR030508). It is a recombinant, His-tagged protein consisting of Met1-Ser740 of human ACE2 (GenBank accession; [NP_068576.1](#)) expressed from HEK293 cells. According to the manufacturer, the protein has a purity of over 95% as determined by SDS/PAGE.

The RBD^{CoV2b} and S477D-RBD^{CoV2b} proteins were kindly provided by Jason McLellan and Kaci Erwin (Department of Molecular Biosciences, University of Texas, Austin, USA). The plasmid JSM-1175 used for this expression encodes SARS-CoV-2 RBD + subdomain-1 (residues 319–591) with an N-terminal artificial signal sequence and a C-terminal HRV3C protease cleavage site, a monomeric Fc tag, and an 8×His tag. The amino acid sequence is shown in Fig. 1. Detailed information on protein expression and purification can be found in Wrapp et al. [18].

Dialysis and ITC experiments

Isothermal titration calorimetry measurements were performed at 25 °C and pH 7.4 on a MicroCal PEAQ Isothermal Titration Calorimeter (Malvern Panalytical Ltd.,

Malvern, UK). After the instrument was stabilized at 25 °C, 40 µL of RBD^{CoV1}, RBD^{CoV2} or RBD^{CoV2b} buffered solutions were used to titrate 200 µL of ACE2 buffered solutions (concentration initially approx. 10 times lower than that of RBD) by 19 consecutive injections with an interval of 150 s between each drop and a stirring speed of 750 r.p.m. (each test was repeated a few times). The reference cell was filled with distilled water. Data were fitted using MicroCal PEAQ-ITC analysis software. An initial injection of 0.4 µL was discarded from each data set to remove the effect of titrant diffusion through the syringe tip during the equilibration process. Thermodynamic parameters (binding affinities, enthalpy and entropy changes) were determined by a combination of nonlinear least-squares fitting and the selection of an appropriate model describing the binding interaction under investigation [29]. CaCl₂-EDTA titration was performed to check the instrument and the results were compared with those obtained for the same samples (test kit) using MicroCal. The heat of dilution was subtracted from each injection [30]. All ITC studies were performed after extensive dialysis of proteins against 1 L of buffer at 5 °C. For each ITC assay, the RBDs and hACE2 receptor protein were dialyzed against the same buffer and during the same time period (the buffer was exchanged 4–5 times every 12 h) to ensure that all samples were as pure as possible and fit into the correct buffer to avoid heat changes due to buffer mismatch. Exhaustive dialysis of all proteins was performed in the same container. After dialysis, the RBDs of SARS-CoV-1 and SARS-CoV-2 were concentrated by centrifugation. The concentration of each protein was determined by measuring the UV absorbance at 280 nm using NanoDrop One C spectrophotometer (Waltham, MA, USA). The

SARS-CoV-1	306	RVVP	SGDV	VRF	FP	317																																																									
SARS-CoV-2	319	RVQP	TESI	VRF	FP	330																																																									
SARS-CoV-2 SD1	319	RVQP	TESI	VRF	FP	330																																																									
SARS-CoV-1	318	NITN	LCPF	GEVFNATK	FP	SVYAWERK	KISNCVADYSVLYNSTF	FSTFKCYGVSATKLN	DLCF	SNV	382																																																				
SARS-CoV-2	331	NITN	LCPF	GEVFNATRF	ASVYAWNR	KRISNCVADYSVLYNSAS	FSTFKCYGVSPTKLN	DLCF	TNV	395																																																					
SARS-CoV-2 SD1	331	NITN	LCPF	GEVFNATRF	ASVYAWNR	KRISNCVADYSVLYNSAS	FSTFKCYGVSPTKLN	DLCF	TNV	395																																																					
SARS-CoV-1	383	YADSF	VVKG	DVRQ	IAPG	QTG	VIADYNYKLPDDF	MGC	VLAWN	TIN	NIDAT	STGN	YK	IR	HR	GK	447																																														
SARS-CoV-2	396	YADSF	VIRG	DEV	RQ	IAPG	QTG	KIADYNYKLPDDF	TG	CVI	AWNS	NNLD	SKV	G	NY	Y	IF	LFR	KSN	460																																											
SARS-CoV-2 SD1	396	YADSF	VIRG	DEV	RQ	IAPG	QTG	KIADYNYKLPDDF	TG	CVI	AWNS	NNLD	SKV	G	NY	Y	IF	LFR	KSN	460																																											
SARS-CoV-1	448	LRP	FERD	IS	NV	PF	SP	DG	K	PCT	-PPA	IN	CV	W	PL	ND	Y	G	F	Y	T	T	T	E	T	E	Y	Q	P	R	V	V	L	S	F	E	L	L	N	A	P	A	T	V	510																		
SARS-CoV-2	461	LK	P	F	E	R	D	I	S	T	E	I	Y	Q	A	G	S	T	P	C	N	G	V	E	G	F	N	C	Y	F	P	L	O	S	Y	G	E	F	O	P	T	N	G	V	Y	Q	P	R	V	V	L	S	F	E	L	L	H	A	P	A	T	V	524
SARS-CoV-2 SD1	461	LK	P	F	E	R	D	I	S	T	E	I	Y	Q	A	G	S	T	P	C	N	G	V	E	G	F	N	C	Y	F	P	L	O	S	Y	G	E	F	O	P	T	N	G	V	Y	Q	P	R	V	V	L	S	F	E	L	L	H	A	P	A	T	V	524
SARS-CoV-1	511	CG	PKL	STD	LI	KN	Q	CV	NF	527																																																					
SARS-CoV-2	525	CG	PKK	ST	NL	V	KN	K	CV	NF	541																																																				
SARS-CoV-2 SD1	525	CG	PKK	ST	NL	V	KN	K	CV	NF	541																																																				
SARS-CoV-2 SD1	542	XF	N	L	T	G	T	G	V	L	T	E	S	N	K	F	L	P	F	Q	Q	F	G	R	D	I	A	D	T	T	D	A	V	R	D	P	Q	T	L	E	I	L	D	I	T	P	C	S	●●●	591													

Fig. 1. Sequence alignment of SARS-CoV-1 S1 RBD, SARS-CoV-2 S1 RBD and SARS-CoV-2 S1 RBD-SD1, named within this work: RBD^{CoV1}, RBD^{CoV2}, and RBD^{CoV2b}, respectively. Residues composing RBD are in magenta. Variable amino acid residues between SARS-CoV-1 and SARS-CoV-2 RBDs are in cyan. The residues of RBD that form bonds with ACE2 are in frames. Orange dots represent monomeric Fc tag.

theoretical extinction coefficients (calculated using Expsy ProtParam) were as follows: 169 180 $\text{M}^{-1}\cdot\text{cm}^{-1}$ for hACE2, and 35 340, 33 850, 91 630 $\text{M}^{-1}\cdot\text{cm}^{-1}$ for RBD^{CoV1}, RBD^{CoV2}, RBD^{CoV2b}, respectively.

Circular dichroism

Circular dichroism (CD) spectra were recorded on a Jasco J-1500 CD spectrometer (Jasco International Co., Tokyo, Japan) in the range 180–350 nm, using a quartz cuvette with an optical path of 0.1 mm. The 10 μL solutions of RBD WT and S477D-RBD were prepared from the solutions of these proteins after dialysis against 20 mM TRIS buffer, pH 7.4, 200 mM NaCl.

Results

Comparison of the thermodynamics of binding of RBD^{CoV1} and RBD^{CoV2} to the hACE2 receptor

After exhaustive dialysis against PBS buffer, pH 7.4, the interactions of RBD^{CoV1} and RBD^{CoV2} with the hACE2 receptor were investigated using ITC. The one-site binding model provided the best fitting values for stoichiometry (N_{ITC}), enthalpy change (ΔH_{ITC}) and an equilibrium constant (K_{dITC}). In this part of our studies, hACE2 at a concentration of 6 μM was in the cell and RBDs (RBD^{CoV1} or RBD^{CoV2} at a concentration of 92 or 91 μM , respectively) were in the syringe. The average data of the two best fits are shown in Table 1. Both receptor binding domains (of SARS-CoV-1 and SARS-CoV-2) bind the hACE2 protein receptor with similar and high affinity and with a stoichiometry ($N_{\text{ITC}} = 1$).

Both systems are enthalpy driven and have very similar ΔG_{ITC} (the change in free energy), as shown in Fig. 2. However, the difference can be seen in the ΔH_{ITC} and ΔS_{ITC} values. When ACE2 interacts with RBD^{CoV2}, both the enthalpic contribution (ΔH_{ITC}) and entropic penalty are larger than when it interacts with RBD^{CoV1} (Table 1). The enthalpy gain of the RBD^{CoV2} interaction is largely compensated by an entropy loss, resulting in no difference in affinity (K_{dITC}).

We hypothesized that the Ser477 residue might be critical for the RBD of SARS-CoV-2 and ACE2 interaction.

Table 1. Differences in the hACE2 receptor binding thermodynamics between RBD of SARS-CoV-1 and RBD of SARS-CoV-2, at pH 7.4 and 25 °C.

	RBD ^{CoV1}	RBD ^{CoV2}
K_{dITC} (nM)	145.5 ± 25.0	144.0 ± 35.3
ΔH_{ITC} (kcal·mol ⁻¹)	-10.50 ± 0.27	-16.15 ± 0.60
N_{ITC}	1.03 ± 0.01	0.99 ± 0.02
$-T\Delta S_{\text{ITC}}$ (kcal·mol ⁻¹)	1.15	6.81

In the Omicron RBD S477 is substituted with N, and that substitution, S477N, has positive impacts on the binding of the Omicron RBD to ACE2 [31]. We were interested if the negatively charged residue (Asp, D) will have opposite impact on RBD to ACE2 binding. The longer fragment of the S protein of SARS-CoV-2 (539 amino acid residues in total, including residues 319–591 of the RBD), named by us RBD^{CoV2b}, was over-expressed for this part of our studies, as described in the methodology section. The S477D mutant of RBD^{CoV2b} was constructed and over-expressed. The RBD^{CoV2b} protein, its S477D mutant and ACE2 were dialyzed against 20 mM TRIS buffer, pH 7.4 + 200 mM NaCl (the buffer was replaced 4–5 times every 12 h). ITC measurements were then performed (Fig. 3) and the results compared. The best-fit values were obtained by nonlinear least-squares analysis of the data to the one-site model. The affinity of the SARS-CoV-2 RBD protein and its S477D mutant to the human ACE2 receptor was very similar ($K_{\text{d}} = 20.1 \pm 2.73 \mu\text{M}$ and $20.2 \pm 4.22 \mu\text{M}$, respectively).

To compare the secondary structures of RBD and its mutant far-UV CD spectroscopy measurements were performed (Fig. 4). Results indicate, that secondary structures of both proteins are rather comparable, with a slightly higher proportion of the alpha-helical structure in S447D-RBD mutant. This observation was also supported by calculations done in k2d3 program.

The influence of Zn(II) ions on the binding of RBD^{CoV2b} to the ACE2 receptor

Next, we wanted to investigate whether the presence of zinc ions in the buffer has an effect on the binding strength and thermodynamic forces of the RBD-ACE2 interaction. On the one hand, the ACE2 protein is known to be a zinc metalloenzyme (PBD: 1R42) and the presence of Zn²⁺ in the buffer might also be necessary to maintain the correct ACE2 structure; on the other hand, there are hypotheses that zinc has anti-coronaviral properties [32,33].

Both interactions are enthalpy driven in buffers with and without zinc ions. Large entropic penalties are observed for both systems, especially for the ACE2-RBD^{CoV2b} interaction studied in the buffer without zinc ions (Table 2 and Fig. 5).

Discussion

Comparison of the thermodynamics of RBD^{CoV1} and RBD^{CoV2} binding to the hACE2 receptor

There are many reports on the binding strength and conformation of the S1-RBD protein during

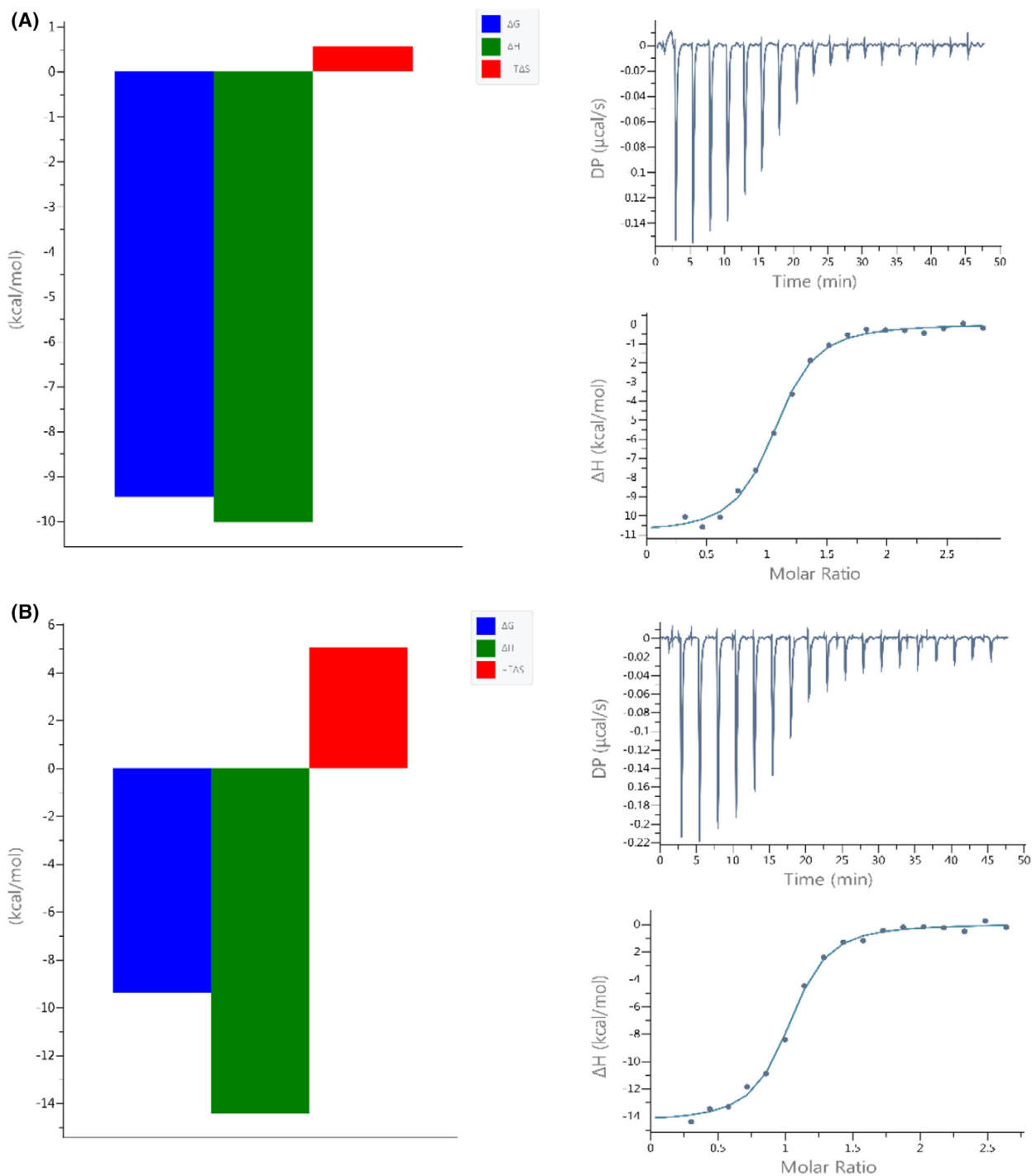


Fig. 2. Signatures (left panels) and calorimetric titration isotherms (right panels) of binding of (A) SARS-CoV-1 RBD and (B) SARS-CoV-2 RBD to the hACE2 receptor protein under the same experimental conditions (PBS buffer, pH 7.4, 25 °C). The concentration of hACE2 was 6 μM and the concentration of the RBDs was in the range of 91–92 μM .

interaction with the human ACE2 receptor, for both SARS-CoV-1 and SARS-CoV-2. However, due to the different techniques used (with variable experimental conditions) and the different S1-RBD

and ACE2 variants studied, it is difficult to compare the binding affinity and other characteristics of ACE2 binding to RBDs of different Betacoronaviruses.

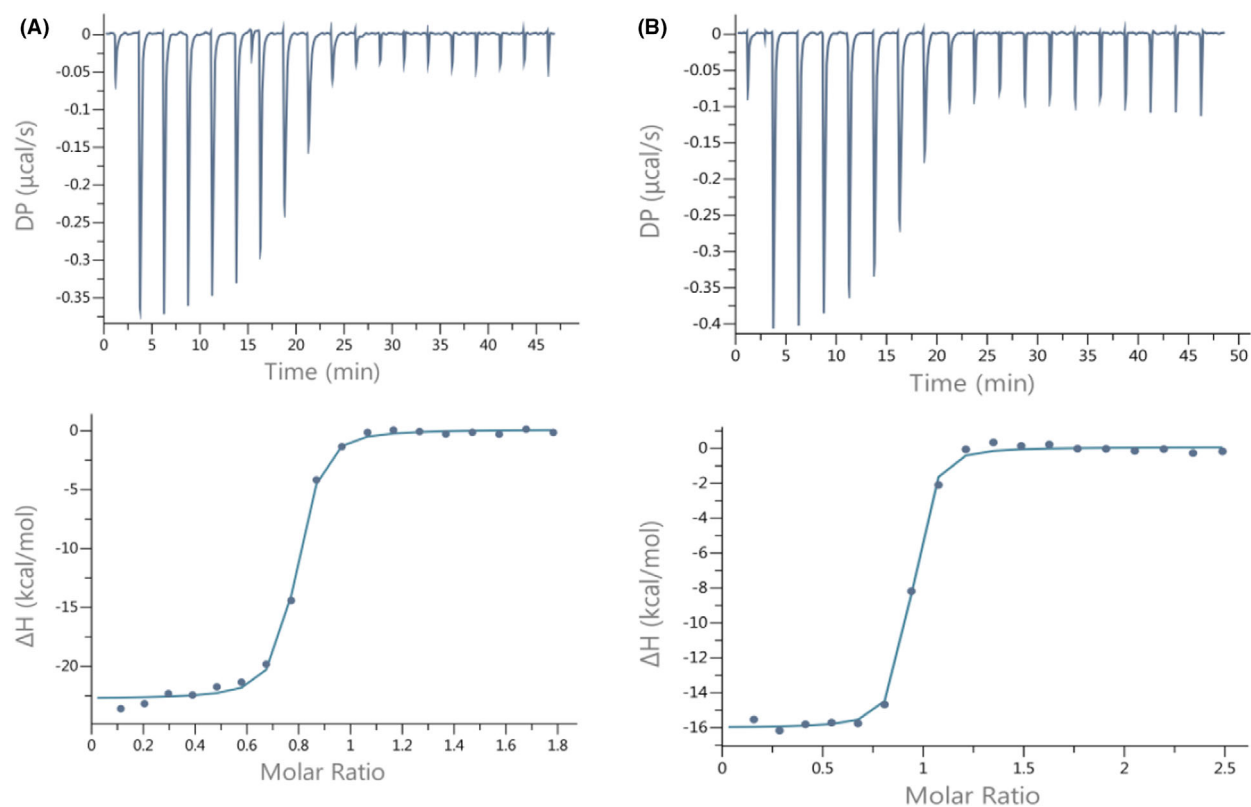


Fig. 3. Calorimetric titration isotherms of binding of (A) wild type SARS-CoV-2 RBD and (B) SARS-CoV-2 RBD mutant (S477D) to the hACE2 receptor protein under the same experimental conditions (TRIS buffer, pH 7.4, 25 °C). The concentration of hACE2 was 9 μM and the concentration of the RBDs was in the range of 86–120 μM .

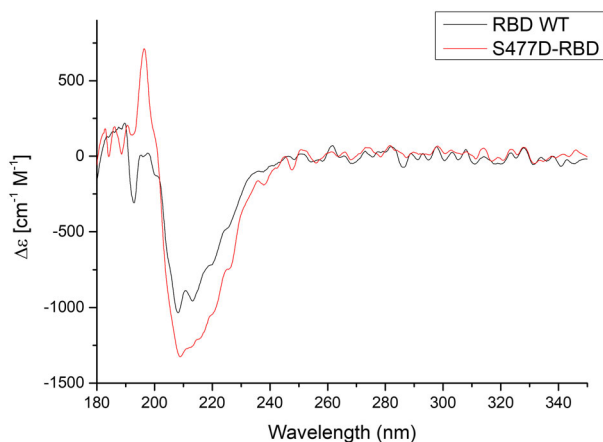


Fig. 4. CD spectra of SARS-CoV-2 RBD (WT) and single amino acid mutation (S477D) in RBD.

Regardless, the interactions of the S1 protein of SARS-CoV-2 and its RBD with the human ACE2 receptor protein have already been studied under variable and not always well-defined conditions. Reported

Table 2. Binding of the ACE2 protein receptor by RBD of SARS-CoV-2, after dialysis of both binding partners in TRIS buffer containing 1 mM Zn^{2+} (left column) and without Zn^{2+} (right column), at pH 7.4 and 25 °C.

	ACE2 – RBD ^{CoV2b} (buffer with Zn^{2+} ions)	ACE2 – RBD ^{CoV2b} (buffer without Zn^{2+} ions)
$K_{d\text{ITC}}$ (nM)	17.9 ± 9.4	15.9 ± 2.3
ΔH_{ITC} (kcal·mol ⁻¹)	-15.2 ± 0.8	-22.15 ± 0.25
N_{ITC}	0.79 ± 0.01	0.83 ± 0.04
$-T_{\Delta S_{\text{ITC}}}$ (kcal·mol ⁻¹)	4.61	11.4

affinity (K_d) values range widely from 1 to 133 nM [17,18,24,34–38]. The S1 protein of SARS-CoV-1 and its binding to the human ACE2 receptor have also been studied. The K_d value of these interactions varied from 5 to 325.8 nM [17–19,39]. These studies were mainly performed with surface plasmon resonance or biolayer interferometry.

In our study, the interactions were investigated under identical experimental conditions. Even dialysis

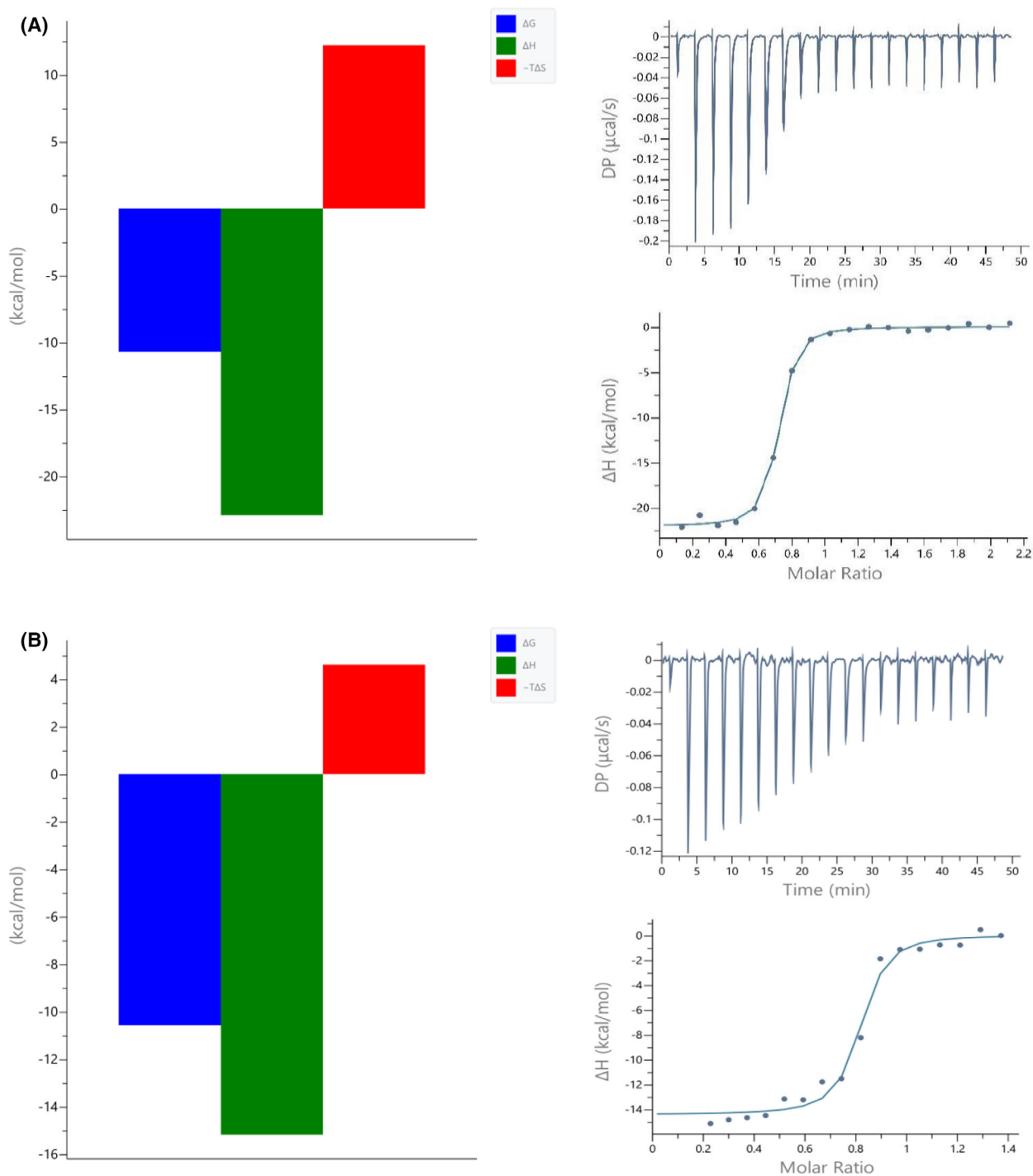


Fig. 5. Signatures (left panels) and calorimetric titration isotherms (right panels) of the binding of $\text{RBD}^{\text{CoV2b}}$ to the hACE2 receptor in buffer without the addition of ZnCl_2 (A) and with the addition of 1 mM Zn^{2+} ions (B). The concentration of hACE2 was $4.5 \mu\text{M}$ and the concentration of the RBD was in the range of $33\text{--}55 \mu\text{M}$.

of all binding partners (RBD^{CoV1} , RBD^{CoV2} and ACE2 proteins) was performed simultaneously in the same buffer. In addition, ITC offers a particular

advantage when measuring protein–protein interactions in solution and without covalent modification of the proteins. To obtain a complete picture of an

interaction, both enthalpic and entropic contributions must be considered, and these were revealed by our studies.

Surprisingly, the RBDs of both viruses bind the ACE2 receptor with very similar affinity (K_{dITC} of 145.5 and 144 nM). However, in the case of the RBD of SARS-CoV-2, a higher enthalpic contribution ($\Delta H_{ITC} = -16.5$) was detected, which was also compensated by a larger entropic disadvantage ($-T\Delta S_{ITC} = 6.81$) than in the case of the RBD^{CoV1}-ACE2 system (Table 1). The more exothermic ΔH could be due to the formation of more energetically favorable non-covalent interactions between RBD^{CoV2} and ACE2.

The valine residue at position 404 in the S protein of SARS-CoV-1 is replaced by a unique residue (Lys417) in the RBD of SARS-CoV-2. As has been shown, unlike Val404 in the RBD of SARS-CoV-1, Lys417 forms salt bridge interactions with Asp30 of ACE2 (Fig. 6) [19].

However, as shown by Lan et al. [19] there are 13 hydrogen bonds and 2 salt bridges at the interface between SARS-CoV-2 and ACE2 compared to 13 hydrogen bonds and 3 salt bridges at the interface between SARS-CoV-1 and ACE2. Moreover, the major contact residues between the RBD of SARS-

CoV-1 and SARS-CoV-2 are largely conserved, suggesting that there may be a different reason for the higher energy of the RBD^{CoV2}-ACE2 interaction than that of the RBD^{CoV1}-ACE2 interaction. Recent work on the interactions of the RBD variants of SARS-CoV-2 with the ACE2 protein showed that only one of the RBD mutations studied (S477N) exhibited an increased enthalpy change [40]. In the RBD of the S protein of SARS-CoV-1, Gly464, which does not bind, corresponds to Ser477 of SARS-CoV-2. We hypothesized that the Ser477 residue may be crucial for the RBD^{CoV2}-ACE2 interaction and responsible for the increased apparent enthalpy change. However, additional ITC studies with the S477D mutant showed that this mutation do not impact affinity to bind ACE2. The far-UV CD spectra of WT RBD and S477D mutant were also similar, what suggest that the mutation do not significantly affect the global structure of RBD.

It is known that sometimes a residue or protein component that does not interact directly with its partner protein can modulate the kinetics and thermodynamics of the molecular recognition process. It has been shown that the region consisting of residues 475–487 is also the key flexible region within the RBM

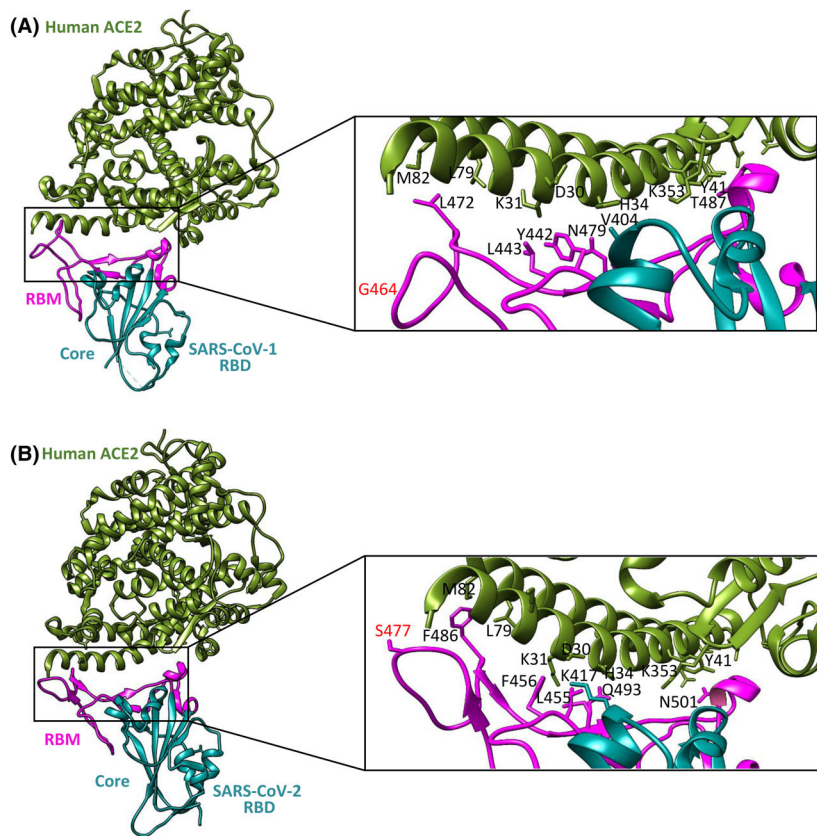


Fig. 6. Comparisons of interactions at the SARS-CoV-1 RBD-ACE2 (A) and the SARS-CoV-2 RBD-ACE2 (B) interfaces. Contacting altered residues are shown as sticks and labeled. ACE2 is green, the core of RBD is in cyan, and RBM is in magenta. PDB ID for SARS-CoV-2 RBD-ACE2 is 6MOJ; PDB ID for SARS-CoV-1 RBD-ACE2 is 2AJF. Visualized by USCF CHIMERA [44].

of the SARS-CoV-2 S protein [41]. The question arises whether the greater entropic disadvantage is due to this region becoming more 'rigid' upon binding of ACE2? It seems likely that this is the case. However, the divergence in the entropy component could be related to the glycan profile of both ACE2 and the RBD of the S protein. The SARS-CoV-2 S protein has a different glycan profile than other coronaviruses [11,42]. Glycans have intrinsic flexibility around glycosidic bonds. For this reason, the loss of conformational entropy of the sugar during protein-protein interaction has thermodynamic consequences that can be captured by ITC. Interestingly, controlled molecular dynamics (SMD) analysis showed that the Asn90 glycan of ACE2 can hinder the association of RBD^{CoV2} with ACE2 more than RBD^{CoV1}, but makes the dissociation of RBD^{CoV2}-ACE2 more difficult than that of RBD^{CoV1}-ACE2 [3].

In summary, it appears that RBD of SARS-CoV-2 has more optimal interaction points, but this interaction leads to greater order in the RBD^{CoV2}-ACE2 complex than RBD^{CoV1}-ACE2, resulting in a more negative ΔS° component.

The influence of Zn²⁺ ions on the binding of RBD^{CoV2b} to the ACE2 receptor

This part of our studies was designed to examine the influence of Zn²⁺ ions on binding with hACE2. We can compare the changes in affinity, enthalpy and entropy between the interaction of RBD^{CoV2b} with the human receptor ACE2 after dialysis in a buffer containing 1 mM Zn²⁺ and without zinc ions because the conditions are almost identical. The results show that the zinc ions present in the buffer have no positive impact on RBD-ACE2.

A slightly higher affinity of RBD to ACE2 studied in buffer without Zn (II) ions (15.9 ± 2.3 nM) and the fact that the process is more enthalpically driven ($\Delta H = -22.15 \pm 0.25$) can be caused by the weak interaction of zinc ions with the TRIS buffer in the second case (Table 2). The Zn(II)-TRIS interaction was shown to have an affinity of 33 mM [43]. Nonetheless, it is quite reasonable to perform such interaction studies in PBS buffer without the addition of zinc ions, as most researchers do.

We are aware that the affinity and thermodynamic properties of the binding of the ACE2-S1 protein do not provide all the information about the interaction of the SARS-CoV-2 virus with the human receptor. Nevertheless, our results provide a solid basis for future studies on SARS-CoV-2 and its mutants. Since the RBM of the S1 protein forms an unstructured loop

(Fig. 6), our future perspective is to design a spike protein fragment containing this loop of SARS-CoV-2 and its variants to identify the unique effects of S1-specific mutations on ACE2 binding. The full thermodynamic properties may provide an answer to the questions of which mutations are central to this interaction and why some of the new variants of SARS-CoV-2 spread more rapidly.

Acknowledgments

The authors thank Kaci Erwin and Jason McLellan at the University of Texas for kindly providing the RBD^{CoV2b} protein and its S477D mutant. This work was supported by a grant from the Polish National Science Centre (UMO-2020/37/B/NZ6/01476).

Conflict of interest

The authors declare no conflict of interest.

Data accessibility

Additional data (e.g., more ITC results) supporting the findings of this study are available from the corresponding author upon request.

Author contributions

AR-B and DW designed the study, conducted the experiments, and wrote the manuscript. AM performed the CD spectroscopy experiments.

References

- 1 Tian F, Tong B, Sun L, Shi S, Zheng B, Wang Z, et al. N501Y mutation of spike protein in SARS-CoV-2 strengthens its binding to receptor ACE2. *Elife*. 2021;**10**:e69091.
- 2 Melanthota SK, Banik S, Chakraborty I, Pallen S, Gopal D, Chakrabarti S, et al. Elucidating the microscopic and computational techniques to study the structure and pathology of SARS-CoVs. *Microsc Res Tech*. 2020;**83**:1623–38.
- 3 Cao W, Dong C, Kim S, Hou D, Tai W, Du L, et al. Biomechanical characterization of SARS-CoV-2 spike RBD and human ACE2 protein-protein interaction. *Biophys J*. 2021;**120**:1011–9.
- 4 Ali A, Vijayan R. Dynamics of the ACE2-SARS-CoV-2/SARS-CoV spike protein interface reveal unique mechanisms. *Sci Rep*. 2020;**10**:14214.
- 5 Raparla S, Li X, Srava JS, Jasti S, Jasti BR. Can structural differences between SARS-CoV and SARS-

- CoV-2 explain differences in drug efficacy? *Curr Trends Biotechnol Pharm.* 2021;**5**:233–40.
- 6 Wang MY, Zhao R, Gao LJ, Gao XF, Wang DP, Cao JM. SARS-CoV-2: structure, biology and structure-based therapeutics development. *Front Cell Infect Microbiol.* 2020;**10**:587269.
 - 7 Stadler K, Masignani V, Eickmann M, Becker S, Abrignani S, Klenk HD, et al. SARS-beginning to understand a new virus. *Nat Rev Microbiol.* 2003;**1**:209–18.
 - 8 Du L, He Y, Zhou Y, Liu S, Zheng BJ, Jiang S. The spike protein of SARS-CoV-a target for vaccine and therapeutic development. *Nat Rev Microbiol.* 2009;**7**:226–36.
 - 9 Sakkiah S, Guo W, Pan B, Ji Z, Yavas G, Azevedo M, et al. Elucidating interactions between SARS-CoV-2 trimeric spike protein and ACE2 using homology modeling and molecular dynamic simulations. *Front Chem.* 2021;**8**:622632.
 - 10 Yan W, Zheng Y, Zeng X, He B, Cheng W. Structural biology of SARS-CoV-2: open the door for novel therapies. *Signal Transduct Target Ther.* 2022;**7**:26.
 - 11 Watanabe Y, Allen JD, Wrapp D, McLellan JS, Crispin M. Site-specific glycan analysis of the SARS-CoV-2 spike. *Science.* 2020;**369**:330–3.
 - 12 Ke Z, Oton J, Qu K, Cortese M, Zila V, McKeane L, et al. Structures and distributions of SARS-CoV-2 spike proteins on intact virions. *Nature.* 2020;**588**:498–502.
 - 13 He Y, Zhou Y, Liu S, Kou Z, Li W, Farzan M, et al. Receptor-binding domain of SARS-CoV spike protein induces highly potent neutralizing antibodies: implication for developing subunit vaccine. *Biochem Biophys Res Commun.* 2004;**324**:773–81.
 - 14 Li W, Moore MJ, Vasilieva N, Siu J, Wong SK, Berne MA, et al. Angiotensin-converting enzyme 2 is a functional receptor for the SARS coronavirus. *Nature.* 2003;**426**:450–4.
 - 15 Wan Y, Shang J, Graham R, Baric RS, Li F. Receptor recognition by the novel coronavirus from Wuhan: an analysis based on decade-long structural studies of SARS coronavirus. *J Virol.* 2020;**94**:e00127-20.
 - 16 Li MY, Li L, Zhang Y, Wang XS. Expression of the SARS-CoV-2 cell receptor gene ACE2 in a wide variety of human tissues. *Infect Dis Poverty.* 2020;**9**:45.
 - 17 Walls AC, Park YJ, Tortorici MA, Wall A, McGuire AT, Veesler D. Structure, function and antigenicity of the SARS-CoV-2 spike glycoprotein. *Cell.* 2020;**180**:281–92.
 - 18 Wrapp D, Wang N, Corbett KS, Goldsmith JA, Hsieh CL, Abiona O, et al. Cryo-EM structure of the 2019-nCoV spike in the prefusion conformation. *Science.* 2020;**367**:1260–3.
 - 19 Lan J, Ge J, Yu J, Shan S, Zhou H, Fan S, et al. Structure of the SARS-CoV-2 spike receptor-binding domain bound to the ACE2 receptor. *Nature.* 2020;**581**:215–20.
 - 20 Yan R, Zhang Y, Li Y, Xia L, Guo Y, Zhou Q. Structural basis for the recognition of SARS-CoV-2 by full-length human ACE2. *Science.* 2020;**367**:1444–8.
 - 21 Li F, Berardi M, Li W, Farzan M, Dormitzer PR, Harrison SC. Conformational states of the severe acute respiratory syndrome coronavirus spike protein ectodomain. *J Virol.* 2006;**80**:6794–800.
 - 22 Song W, Gui M, Wang X, Xiang Y. Cryo-EM structure of the SARS coronavirus spike glycoprotein in complex with its host cell receptor ACE2. *PLoS Pathog.* 2018;**14**:e1007236.
 - 23 Nassar A, Ibrahim IM, Amin FG, Magdy M, Elgharib AM, Azzam EB, et al. A review of human coronaviruses' receptors: the host-cell targets for the crown bearing viruses. *Molecules.* 2021;**26**:6455.
 - 24 Shang J, Ye G, Shi K, Wan Y, Luo C, Aihara H, et al. Structural basis of receptor recognition by SARS-CoV-2. *Nature.* 2020;**581**:221–4.
 - 25 Adhikari P, Li N, Shin M, Steinmetz NF, Twarock R, Podgornik R, et al. Intra- and intermolecular atomic-scale interactions in the receptor binding domain of SARS-CoV-2 spike protein: implication for ACE2 receptor binding. *Phys Chem Chem Phys.* 2020;**22**:18272–83.
 - 26 Wang Q, Zhang Y, Wu L, Niu S, Song C, Zhang Z, et al. Structural and functional basis of SARS-CoV-2 entry by using human ACE2. *Cell.* 2020;**181**:894–904.
 - 27 Xie Y, Karki CB, Du D, Li H, Wang J, Sobitan A, et al. Spike proteins of SARS-CoV and SARS-CoV-2 utilize different mechanisms to bind with human ACE2. *Front Mol Biosci.* 2020;**7**:591873.
 - 28 Dorowski S, Szwamel K. Paramedics' knowledge of medical guidelines and procedures for protection against coronavirus during the COVID-19 pandemic: a pilot study. *Med Sci Pulse.* 2021;**4**:19–26.
 - 29 Turnbull WB, Daranas AH. On the value of c: can low affinity systems be studied by isothermal titration calorimetry? *J Am Chem Soc.* 2003;**125**:14859–66.
 - 30 Grosseohme NE, Spuches AM, Wilcox DE. Application of isothermal titration calorimetry in bioinorganic chemistry. *J Biol Inorg Chem.* 2010;**5**:1183–91.
 - 31 Lan J, He X, Ren Y, Wang Z, Zhou H, Fan S, et al. Structural insights into the SARS-CoV-2 omicron RBD-ACE2 interaction. *Cell Res.* 2022;**32**(6):593–5.
 - 32 Salgo MP. COVID-19 – zinc and angiotensin-converting enzyme 2 (ACE2) deficiencies as determinants of risk and severity of disease: a narrative review. *Infect Dis Ther.* 2021;**10**:1215–25.
 - 33 Hecel A, Ostrowska M, Stokowa-Sołtys K, Wąty J, Dudek D, Miller A, et al. Zinc(II)—the overlooked éminence grise of chloroquine's fight against COVID-19? *Pharmaceuticals.* 2020;**13**:228.
 - 34 Lei C, Qian K, Li T, Zhang S, Fu W, Ding M, et al. Neutralization of SARS-COV-2 spike pseudotyped

- virus by recombinant ACE2-Ig. *Nat Commun.* 2020;**11**:2070.
- 35 Supasa P, Zhou D, Dejnirattisai W, Liu C, Mentzer AJ, Ginn HM, et al. Reduced neutralization of SARS-CoV-2b.1.1.7 variant by convalescent and vaccine sera. *Cell.* 2021;**184**:2201–11.
- 36 Zhang J, Cai Y, Xiao T, Lu J, Peng H, Sterling SM, et al. Structural impact on SARS-CoV-2 spike protein by D614G substitution. *Science.* 2021;**372**:525–30.
- 37 Laffeber C, de Koning K, Kanaar R, Lebbink JHG. Experimental evidence for enhanced receptor binding by rapidly spreading SARS-CoV-2 variants. *J Mol Biol.* 2021;**433**:167058.
- 38 Barton MI, MacGowan SA, Kutuzov MA, Dushek O, Barton GJ, van der Merwe PA. Effects of common mutations in the SARS-CoV-2 spike RBD and its ligand, the human ACE2 receptor on binding affinity and kinetics. *Elife.* 2021;**10**:e70658.
- 39 Kirchdoerfer RN, Wang N, Pallesen J, Wrapp D, Turner HL, Cotrell CA, et al. Stabilized coronavirus spikes are resistant to conformational changes induced by receptor recognition or proteolysis. *Sci Rep.* 2018;**8**:15701.
- 40 Upadhyay V, Lucas A, Panja S, Miyauchi R, Mallela KMG. Receptor binding, immune escape, and protein stability direct the natural selection of SARS-CoV-2 variants. *J Biol Chem.* 2021;**297**:101208.
- 41 Singh A, Steinkellner G, Köchl K, Gruber K, Gruber CC. Serine 477 plays a crucial role in the interaction of the SARS-CoV-2 spike protein with the human receptor ACE2. *Sci Rep.* 2021;**11**:4320.
- 42 Witkowska D. Mass spectrometry and structural biology techniques in the studies on the coronavirus-receptor interaction. *Molecules.* 2020;**25**:4133.
- 43 Bologni L, Sabatini A, Vecca A. Complex formation equilibria between 2-amino-2(hydroxymethyl)-1,3,-propanediol (tris, tham) and nickel(II), copper(II), zinc (II) and hydrogen ions in aqueous solutions. *Inorg Chim Acta.* 1983;**69**:71–5.
- 44 Pettersen EF, Goddard TD, Huang CC, Couch GS, Greenblatt DM, Meng EC, et al. UCSF Chimera—a visualization system for exploratory research and analysis. *J Comput Chem.* 2004;**25**:1605–12.